Am. J. Hum. Genet. 73:926–932, 2003

Report

Slowed Conduction and Thin Myelination of Peripheral Nerves Associated with Mutant Rho Guanine-Nucleotide Exchange Factor 10

Kristien Verhoeven,[1] Peter De Jonghe,[1,3] Tom Van de Putte,[4] Eva Nelis,[1] An Zwijsen,[4] Nathalie Verpoorten,[1] Els De Vriendt,[1] An Jacobs,[1] Veerle Van Gerwen,[1] Annick Francis,[4] Chantal Ceuterick,[2] Danny Huylebroeck,[4] and Vincent Timmerman[1]

[1]Molecular Genetics Department, Flanders Interuniversity Institute for Biotechnology, and [2]Laboratory of Neuropathology and Electronmicroscopy, Born-Bunge Foundation (BBS), University of Antwerp, and [3]Division of Neurology, University Hospital of Antwerp, Antwerp; and [4]Developmental Biology Department, Flanders Interuniversity Institute for Biotechnology, University of Leuven, Leuven, Belgium

Slowed nerve-conduction velocities (NCVs) are a biological endophenotype in the majority of the hereditary motor and sensory neuropathies (HMSN). Here, we identified a family with autosomal dominant segregation of slowed NCVs without the clinical phenotype of HMSN. Peripheral-nerve biopsy showed predominantly thinly myelinated axons. We identified a locus at 8p23 and a Thr109Ile mutation in *ARHGEF10*, encoding a guanine-nucleotide exchange factor (GEF) for the Rho family of GTPase proteins (RhoGTPases). Rho GEFs are implicated in neural morphogenesis and connectivity and regulate the activity of small RhoGTPases by catalyzing the exchange of bound GDP by GTP. Expression analysis of ARHGEF10, by use of its mouse orthologue Gef10, showed that it is highly expressed in the peripheral nervous system. Our data support a role for ARHGEF10 in developmental myelination of peripheral nerves.

The phenotype of slowed motor and sensory nerve-conduction velocities (NCVs) in a 4-generation family (De Jonghe et al. 1999) was accidentally discovered on clinical and electrophysiological examination of proband III-16 for vascular problems of the leg. Subsequent examination identified slowed NCVs in 12 of 39 healthy relatives (5 males and 7 females), indicating an autosomal dominant inheritance of the phenotype (fig. 1*A*). NCVs were uniformly slowed in all nerves examined; 34–42 m/s for motor median nerve (normal ⩾49 m/s), 27–36 m/s for motor peroneal nerve (normal ⩾41 m/s), 32–46 m/s for sensory median nerve (normal ⩾46 m/s), 33–45 m/s for sensory ulnar nerve (normal ⩾46 m/s), and 28–35 m/s for sensory sural nerve (normal ⩾44 m/s). Compound muscle-action potentials were normal, and sensory nerve–action potentials were sometimes slightly reduced. None of the affected family members showed any clinical signs of peripheral or CNS dysfunction. The eldest individuals, II-4 and II-7 (aged 87 and 78 years, respectively, at time of neurological examination), had NCVs that were not significantly different from those measured in younger affected individuals. Histological studies of a peripheral-nerve biopsy of proband III-16 at age 54 years showed numerous relatively thin myelin sheaths (mean *g*-ratio: 0.75 for myelinated fibers, with a range of 2–7 μm) (fig. 1*B*), slight onion-bulb formation, and few axonal-regeneration clusters (De Jonghe et al. 1999).

We performed a 10-cM density genomewide linkage analysis and obtained a conclusive linkage with D8S264 on chromosome 8p23 (table 1). The region around D8S264 was saturated with known and novel microsatellite markers, and a maximum LOD score of 9.33, at recombination fraction (θ) 0, was calculated with marker AF009213 (table 1). Haplotype analysis identified meiotic recombinants, with STR2 and D8S504 restricting the candidate region to 1.5 Mb, on the basis of sequence contigs NT_008060, NT_037694, and NT_023744 (NCBI, LocusLink) (fig. 2*a*). Within the sequence, a total of five known genes was identified, which

Received May 2, 2003; accepted for publication June 23, 2003; electronically published August 19, 2003.

Address for correspondence and reprints: Dr. Vincent Timmerman, Department of Molecular Genetics (VIB8), Peripheral Neuropathy Group, University of Antwerp, Universiteitsplein 1, B-2610 Antwerp, Belgium. E-mail: vincent.timmerman@ua.ac.be

0002-9297/2003/7304-0018$15.00

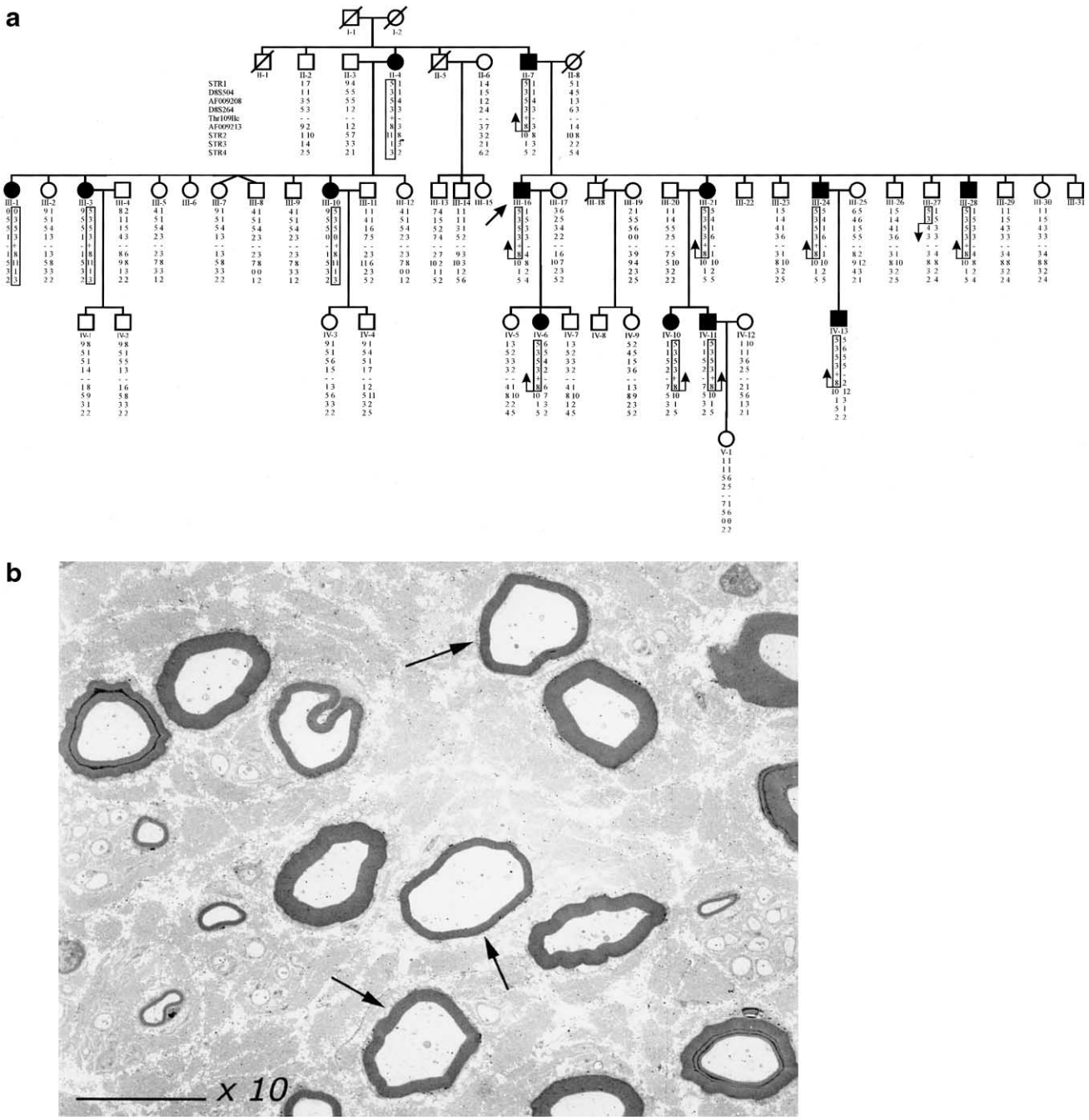

Figure 1 Haplotype analysis of chromosome 8p23 STR markers. *a,* Pedigree of the family with slowed NCVs. Squares = male; circles = female; unblackened = unaffected; blackened = reduced nerve conduction phenotype; slashed = deceased; diagonal arrow = proband. Blood samples were obtained after informed consent and approval of the Committee for Medical Ethics, University of Antwerp. A genomewide scan was performed using 382 STR markers from the ABI Prism Linkage Mapping, Set MD-10 (Applied Biosystems). Conclusive linkage was found with D8S264. Additional STR markers were used in the fine mapping: three known markers (D8S504, AF009208, and AF009213) and four novel STR markers (designated "STR1," "STR2," "STR3," and "STR4") (table A [online only]). Genotypes are represented by allele numbers; "0 0" = failed genotype. For each STR marker, a disease haplotype was constructed (*box*). The presence of the Thr109Ile mutation is indicated by a plus sign (+), the absence by a minus sign (−). The meiotic recombination events, indicated with an arrow, assign the disease locus to the chromosome segment contained between D8S504 and STR2. *b,* Electron microscopy. Transverse section of superficial fibular nerve shows thinly myelinated fibers (*arrows*). Scale bar = 10 μm.

Table 1

Two-Point Linkage Results with Chromosome 8p23 Markers

	LOD AT θ =							
MARKER	0	.001	.01	.05	.1	.2	.3	.4
STR1	6.32	6.31	6.22	5.81	5.26	4.05	2.68	1.19
D8S504	−∞	6.20	7.07	7.20	6.76	5.44	3.79	1.87
AF009208	6.98	6.97	6.87	6.41	5.82	4.58	3.19	1.60
D8S264	3.01	3.01	2.96	2.77	2.51	1.95	1.34	.68
Thr109Ile	9.93	9.91	9.78	9.17	8.37	6.64	4.68	2.46
AF009213	9.33	9.32	9.19	8.60	7.82	6.14	4.24	2.09
STR2	−∞	4.39	5.28	5.51	5.19	4.15	2.84	1.34
STR3	−∞	4.27	5.18	5.44	5.18	4.25	3.02	1.53
STR4	−∞	5.36	6.25	6.43	6.05	4.90	3.44	1.72

NOTE.—Two-point linkage analysis was performed with the MLINK program of the FASTLINK program package (Lathrop and Lalouel 1984; Cottingham et al. 1993). Since NCV values were diagnostic in all individuals, the phenotype was coded as a 100% penetrant phenotype (De Jonghe et al. 1999). The gene frequency was set at 0.0001, allele frequencies were set at $1/N$ (N = number of alleles observed in the pedigree), and equal recombination rates between males and females were assumed. (Sequences of the four new STR markers [STR1, STR2, STR3, and STR4] shown in table A [online only].)

we analyzed for mutations by genomic sequencing of exons and flanking splice sites in two affected individuals and two control individuals: KIAA0711 (hypothetical protein KIAA0711 [GenBank accession number NM_014867]), *MYOM2* (myomesin [M-protein] 2 [GenBank accession number NM_003970]), *CLN8* (ceroid-lipofuscinosis, neuronal 8 [GenBank accession number NM_018941]), *DLGAP2* (discs, large [*Drosophila*] homolog-associated protein 2 [GenBank accession number NM_004745]), and *ARHGEF10* (Rho guanine-nucleotide exchange [GEF] factor 10 [GenBank accession number NM_014629]) (intronic primers for ARHGEF10 shown in table B [online only]). A heterozygous mutation, C→T (c.326C→T; g.6110C→T), was observed in exon 3 of *ARHGEF10,* encoded by 22 exons, as shown by sequence alignment of its 8,467-bp transcript (GenBank accession number NM_014629), with the genomic sequence contained in NT_023744 (fig. 2*b*). The presence of the mutation was confirmed by *Ban*I digestion of PCR-amplified exon 3, generating one mutant fragment of 329 bp and two wild-type fragments of 172 bp and 157 bp. Complete cosegregation of the mutation was observed in the family (LOD = 9.93) (fig. 1; table 1), and the mutation was absent in 600 control chromosomes. The mutation predicts an amino acid substitution of threonine (Thr) to isoleucine (Ile) at codon 109 (Thr109Ile) of the ARHGEF10 protein (GenBank accession number NP_055444). Clustal W protein alignment of the human ARHGEF10 protein—with its orthologues in macaque (GenBank accession number BAB12119), puffer fish (GenBank accession number FuguGenscan_7637), and mouse (Gef10) (GenBank accession number NP_766339)—showed that Thr109 is a conserved amino acid in all four species (table C [online only]). Screening of patients with different clinical subtypes of Charcot-Marie-Tooth disease did not identify mutations in *ARHGEF10*. This is not unexpected, given that the individuals in our family were clinically unaffected and had minor disturbances in NCVs and myelination.

We examined expression of *ARHGEF10,* using its mouse orthologue, *Gef10*. Alignment of the *Gef10* transcript of 4,481 bp (GenBank accession number NM_172751) with the genomic sequence NT_039455 identified 24 exons; exons 1 and 2 were absent from *ARHGEF10* (fig. 2*b*). Multiple-tissue northern blot analysis of *Gef10* indicated ubiquitous expression (data not shown). Overlapping primer sets covering the mouse cDNA sequence were used in PCR analysis on cDNA of E13 mouse brain, dorsal root ganglia (DRG), and ventral horn (VH) and demonstrated *Gef10* expression in all three neuronal tissues. Extra PCR fragments that indicated the presence of alternative transcripts were observed (fig. 2*c*–2*e*). Sequencing of these fragments identified three splice variants of *Gef10*: one in all three tissues missing exon 4 (fig. 2*c*), one specific for DRG missing exon 21 (fig. 2*d*), and one specific to VH, with an insertion of an additional exon of 165 bp between exons 22 and 23 (fig. 2*e*). Exon 5, which corresponds to exon 3 in *ARHGEF10* and contains the Thr109Ile mutation, is present in all three variant transcripts. Whole-mount in situ hybridization experiments in mouse embryos at E8.5 showed *Gef10* expression in the neuroepithelium of the meninges, including the optic sulcus (fig. 3*a* and 3*b*). At E9.5, high levels of *Gef10* expression were detected in the roof plate of the rhombencephalon (fig. 3*c* and 3*d*). In E12.5 embryos, Gef10 is ubiquitously expressed, with a pronounced expression in the neuroepithelium of brain vesicles, the neural tube, the ganglia, DRG, and the neural layer of retina (fig. 3*e*–3*h*).

ARHGEF10 encodes a guanine-nucleotide exchange factor for the Rho family of GTPase proteins (RhoGEFs) and contains a Dbl homology (DH) domain (codons 177–359), a common feature of all RhoGEFs (Zheng 2001). RhoGEFs activate RhoGTPases by catalyzing the exchange of bound GDP for GTP, which induces a conformational change in the GTP-bound GTPase that allows its interaction with downstream effector proteins (Bourne et al. 1990; Boguski and McCormick 1993; Hart et al. 1994). Within the RhoGEF family, DH domains are invariably followed by a pleckstrin homology (PH) domain, supposed to be involved in subcellular localization of RhoGEFs (Hoffman and Cerione 2002). However, in ARHGEF10, we could not detect a PH-domain consensus motif using several bioinformatic tools (BlastP, ScanProsite, or InterPro). So far, only one

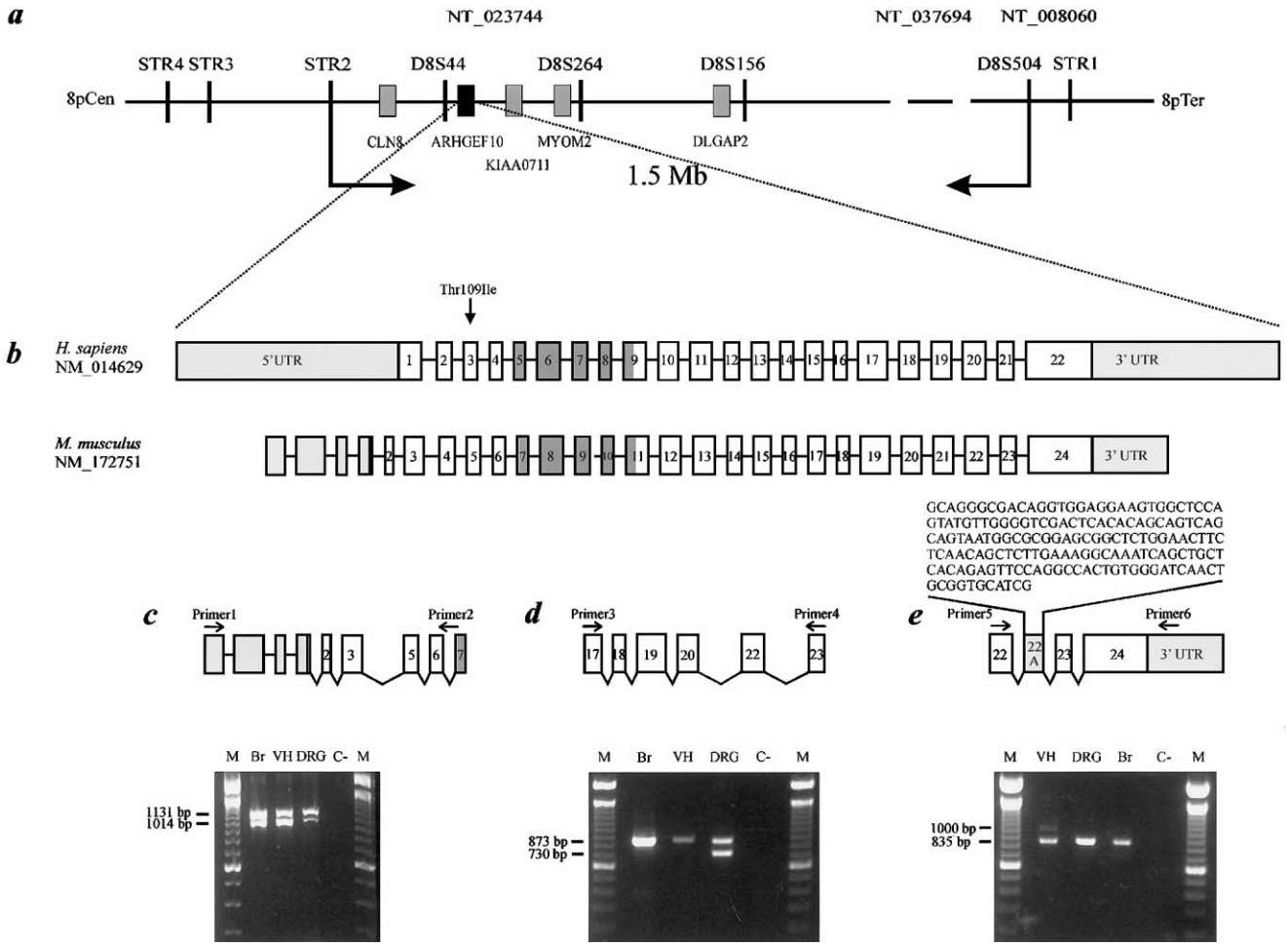

Figure 2 Positional cloning and expression analysis of *ARHGEF10*. *a,* Linked region on chromosome 8p23. Meiotic recombinants with STR2 and D8S504 defined a critical region of 1.5 Mb. Shaded boxes indicate the five known genes in the region. *b,* Genomic structure of human *ARHGEF10* and mouse *Gef10,* aligned. The 5′ and 3′ UTRs are light gray; the Dbl domain is dark gray. An arrow indicates the position of the Thr109Ile mutation. *c–e,* Expression analysis of mouse *Gef10* on cDNA of motor and sensory neurons isolated from VH and DRG of mice embryos, age 13 d. Expression analysis was performed with oligonucleotide primer pairs spread over the proximal, middle, and distal part of the gene. Subsequent direct-DNA sequencing analysis of PCR fragments was performed. M = 100-bp size marker (Invitrogen); Br = mouse brain cDNA (Clontech); VH = VH cDNA; DRG = DRG cDNA; C− = blanco. *c,* cDNA primer1 and primer2, splicing of exon 4 in the smaller fragment in brain, VH, and DRG. *d,* cDNA primer3 and primer4, skipping of exon 21 in DRG. *e,* cDNA primer5 and primer6, additional exon identified, located between exon 22 and 23 in VH. (Primer sequences shown in table D [online only].)

other mammalian RhoGEF family member, p164-RhoGEF, lacking the PH domain has been reported (Rumenapp et al. 2002). ARHGEF10 appears to lack an equivalent protein in *Caenorhabditis elegans*, *Drosophila melanogaster*, *Dictyostelium discoideum,* and *Saccharomyces cerevisiae,* which suggests that the ARHGEF10 signaling pathway is unique to vertebrates. This confirms the overall picture of plasticity, when comparing the RhoGTPases and their interacting proteins between species, with certain species gaining or losing RhoGTPase and RhoGEF family members to give rise to unique sets of signaling proteins (Wherlock and Mellor 2002). RhoGTPases play a pivotal role in regulating the actin cytoskeleton, but their ability to influence cell polarity, microtubule dynamics, membrane-transport pathways, and transcription-factor activity is probably just as significant (Etienne-Manneville and Hall 2002). Recent evidence has implicated RhoGTPases in neuronal morphogenesis, including cell migration, axonal growth and guidance, dendrite elaboration and plasticity, and synapse formation. Several GEFs play a central role in defining the temporal and spatial activation of the corresponding GTPase within neuronal cells (Etienne-Manneville and Hall 2002).

Here, we report a Thr109Ile mutation in *ARHGEF10* cosegregating with slowed NCVs of peripheral nerves

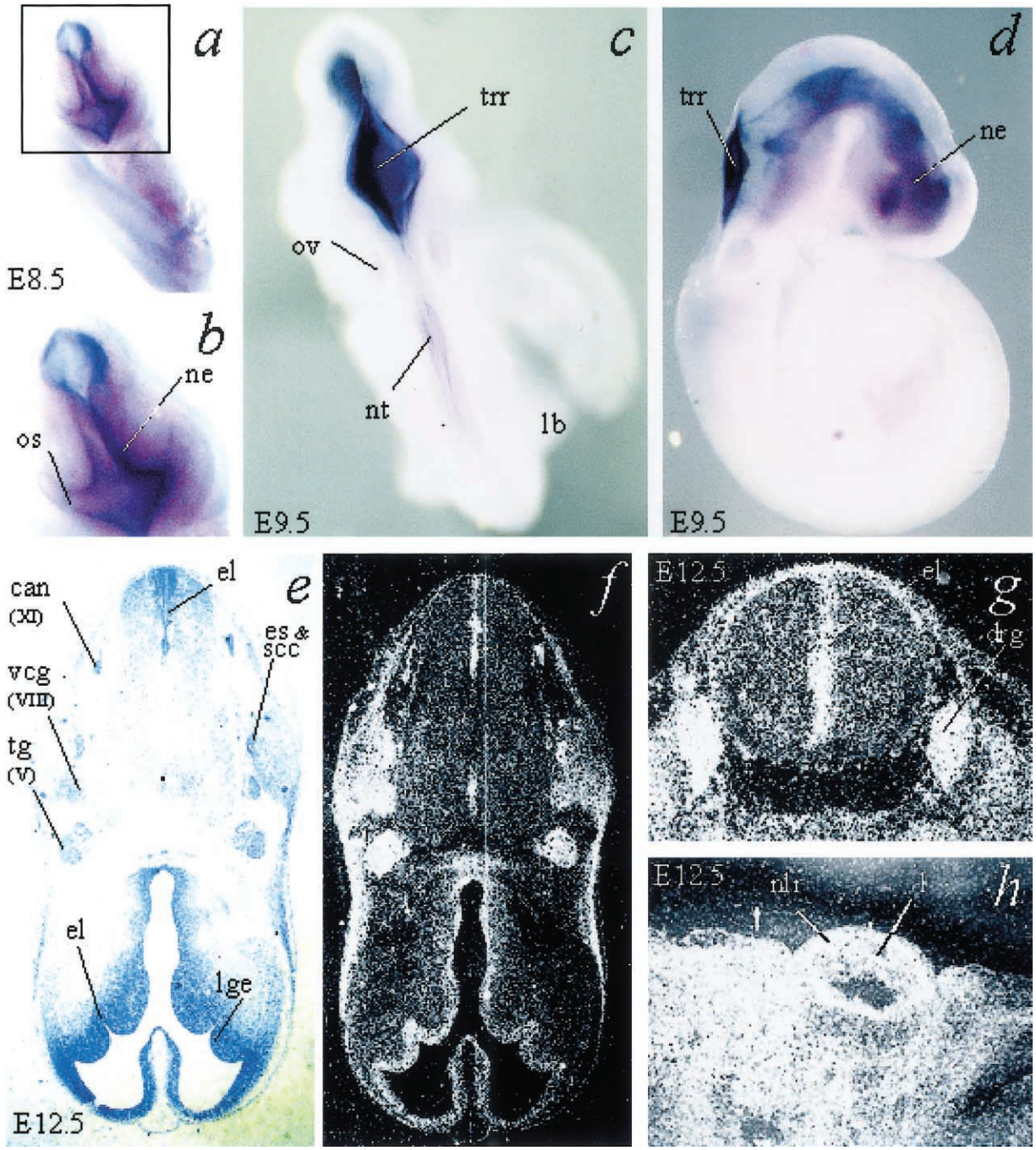

Figure 3 Expression pattern of *Gef10* mRNA in mouse embryo. *a* and *b*, Frontal view on an E8.5 embryo (*a*) and blowup of the head region (*b*) hybridized with the *GEF10* probe. *GEF10* mRNA is expressed in the neuroepithelium (ne) of brain vesicles and optic stalk (os). *c* and *d*, Dorsal (*c*) and lateral (*d*) views on an E9.5 embryo. High levels of *GEF10* mRNA are observed in the thin roof of the rhombencephalon (trr), the neuroepithelium lining the brain ventricles, and, to a lesser extend, in the neural tube (nt). *e–h*, Bright-field (*e*) and corresponding dark-field image (*f*) of a transversal section at the level of the epithalamus of E12.5 embryo. Transcripts of *GEF10* are present in the ependymal layer (el) of neural tube and brain vesicles, as well as in the trigeminal ganglia (tg) of the head. *GEF10* transcripts are also detected in the endolymphatic sac (es) and semicircular canal (ssc). *g*, Dark-field image of a transversal section through the neural tube. Note high expression in the ependymal layer of the neural tube and the DRG. *h*, Transversal section through the region of the eye at E12.5, revealing very high *GEF10* expression levels in the neural layer of the retina (nlr). can(XI) = cranial accessory (XI) nerve; tg(V) = trigeminal (V) ganglion; vcg(VIII) = vestibulocochlear (VIII) ganglion; ov = otic vesicle; l = lens; lge = lateral ganglionic eminence; lb = limb bud. The whole-mount and radioactive in situ hybridizations were performed as reported elsewhere (Wilkinson 1992; Dewulf et al. 1995).

without clinical phenotype in a 4-generation family. RhoGEFs have been implicated elsewhere in human genetic disorders. A mutation in the DH domain of *FGD1 GEF* cosegregates with faciogenital dysplasia, a developmental disorder (Pasteris et al. 1994). Mutations in *ARHGEF6* (also known as "*αPIX*") are associated with X-linked nonsyndromic mental retardation (Kutsche et al. 2000). Loss-of-function mutations in the *ALS2* (*alsin*) gene cause autosomal recessive amyotrophic lateral sclerosis (ALS2), a neurodegenerative disorder affecting the large motor neurons of the CNS (Hadano et al. 2001; Yang et al. 2001). The identification of *ARHGEF10* as a gene implicated in peripheral-nerve conduction raises questions about its role during the development of the peripheral nervous system in vertebrates. All affected individuals in the family had slowed NCVs with normal amplitudes at all ages, which indicates that the phenotype is nonprogressive. Together with the numerous thin myelinated axons in the absence of gross signs of demyelination or axonal degeneration and regeneration in the peripheral nerve biopsy of the proband, these observations are indicative of a congenital nonprogressive phenotype, which suggests that *ARHGEF10* is most likely involved in normal development of peripheral nerves, though its actual biological function remains to be elucidated. Also, the upstream signaling cascade necessary for ARHGEF10 activation and the RhoGTPase subsequently activated by ARHGEF10 remain to be clarified.

Acknowledgments

The authors gratefully acknowledge the cooperation and participation of all family members in this study and the contribution of the Flanders Interuniversity Institute for Biotechnology Genetic Service Facility in the genetic analyses. We also thank Christine Van Broeckhoven for critical reading of the manuscript and helpful discussions. This research project was supported by the Fund for Scientific Research (FWO-Flanders), special research funds of the University of Antwerp, the Medical Foundation Queen Elisabeth, the Association Belge contre les Maladies Neuro-Musculaires, and the Interuniversity Attraction Poles programme P5/19 of the Federal Office for Scientific, Technical and Cultural Affairs Belgium. K.V., A.Z., and E.N. are postdoctoral fellows of the FWO-Flanders. N.V. is supported by a Ph.D. fellowship of the Institute for Science and Technology, Belgium.

Electronic-Database Information

Accession numbers and URLs for data presented herein are as follows:

Clustal W, http://npsa-pbil.ibcp.fr/cgi-bin/npsa_automat.pl?page=/NPSA/npsa_server.html (for multiple protein alignment)

GenBank, http://www.ncbi.nlm.nih.gov/entrez/query.fcgi?db=Nucleotide (for mRNA sequences: MYOM2 [accession number NM_003970], KIAA0711 [accession number NM_014867], GEF10 [ARHGEF10] [accession number NM_014629], CLN8 [accession number NM_018941] DLGAP2 [accession number NM_004745], *Homo sapiens* RhoGEF10 [accession number NP_055444], and *Mus musculus* RIKEN cDNA [accession number NM_172751])

NCBI Map Viewer, http://www.ncbi.nlm.nih.gov/mapview/

ScanProsite, http://us.expasy.org/cgi-bin/scanprosite

References

Boguski MS, McCormick F (1993) Proteins regulating Ras and its relatives. Nature 366:643–654

Bourne, HR, Sanders DA, McCormick F (1990) The GTPase superfamily: a conserved switch or diverse cell functions. Nature 348:125–132

Cottingham RW Jr, Idury RM, Schäffer AA (1993) Faster sequential genetic linkage computations. Am J Hum Genet 53: 252–263

De Jonghe P, Timmerman V, Nelis E, De Vriendt E, Löfgren A, Ceuterick C, Martin J-J, Van Broeckhoven C (1999) A novel type of hereditary motor and sensory neuropathy characterised by a mild phenotype. Arch Neurol 56:1283–1288

Dewulf N, Verschueren K, Lonnoy O, Moren A, Grimsby S, Van de Spiegle K, Miyazono K, Huylebroeck D, Ten Dijke P (1995) Distinct spatial and temporal expression patterns of two type I receptors for bone morphogenetic proteins during mouse embryogenesis. Endocrinology 136:2652–2663

Etienne-Manneville S, Hall A (2002) Rho GTPases in cell biology. Nature 420:629–635

Hadano S, Hand CK, Osuga H, Yanagisawa Y, Otomo A, Devon RS, Miyamoto N, Showguchi-Miyata J, Okada Y, Singaraja R, Figlewicz DA, Kwiatkowski T, Hosler BA, Sagie T, Skaug J, Nasir J, Brown RH Jr, Scherer SW, Rouleau GA, Hayden MR, Ikeda JE (2001) A gene encoding a putative GTPase regulator is mutated in familial amyotrophic lateral sclerosis 2. Nat Genet 29:166–173

Hart MJ, Eva A, Zangrilli D, Aaronson SA, Evans T, Cerione RA, Zheng Y (1994) Cellular transformation and guanine nucleotide exchange activity are catalyzed by a common domain on the dbl oncogene product. J Biol Chem 269:62–65

Hoffman GR, Cerione RA (2002) Signaling to the Rho GTPases: networking with the DH domain. FEBS Lett 513:85–91

Kutsche K, Yntema H, Brandt A, Jantke I, Nothwang HG, Orth U, Boavida MG, David D, Chelly J, Fryns JP, Moraine C, Ropers HH, Hamel BC, van Bokhoven H, Gal A (2000) Mutations in ARHGEF6, encoding a guanine nucleotide exchange factor for Rho GTPases, in patients with X-linked mental retardation. Nat Genet 26:247–250

Lathrop, GM, Lalouel JM (1984) Easy calculations of lod scores and genetic risk on small computers. Am J Hum Genet 36:460–465

Pasteris NG, Cadle A, Logie LJ, Porteous ME, Schwartz CE, Stevenson RE, Glover TW, Wilroy RS, Gorski JL (1994) Isolation and characterization of the faciogenital dysplasia (Aarskog-Scott syndrome) gene: a putative Rho/Rac guanine nucleotide exchange factor. Cell 79:669–678

Rumenapp U, Freichel-Blomquist A, Wittinghofer B, Jakobs

KH, Wieland T (2002) A mammalian Rho-specific guanine-nucleotide exchange factor (p164-RhoGEF) without a pleckstrin homology domain. Biochem J 366:721–728

Wherlock M, Mellor H (2002) The Rho GTPase family: a Racs to Wrchs story. J Cell Sci 115:239–240

Wilkinson DG (1992) Whole mount in situ hybridization of vertebrate embryos. In: Wilkinson DG (ed) In situ hybridization: a practical approach. IRL Press, Oxford, United Kingdom, pp 75–84

Yang Y, Hentati A, Deng HX, Dabbagh O, Sasaki T, Hirano M, Hung WY, Ouahchi K, Yan J, Azim AC, Cole N, Gascon G, Yagmour A, Ben Hamida M, Pericak-Vance M, Hentati F, Siddique T (2001) The gene encoding alsin, a protein with three guanine-nucleotide exchange factor domains, is mutated in a form of recessive amyotrophic lateral sclerosis. Nat Genet 29:160–165

Zheng Y (2001) Dbl family guanine nucleotide exchange factors. Trends Biochem Sci 26:724–732